

# Molecular Dipole Layer and Alkyl Side-Chain Induced Improvement in the Energy Level Alignment and Wetting of Dinaphthothienothiophene Thin Films

Subhankar Mandal, Souvik Jana, Saugata Roy, Md Saifuddin, and Satyajit Hazra\*



Cite This: *J. Phys. Chem. C* 2023, 127, 18176–18184



Read Online

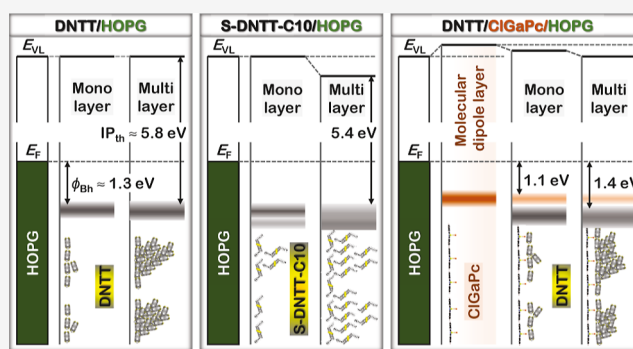
ACCESS |

Metrics & More

Article Recommendations

Supporting Information

**ABSTRACT:** The evolution of electronic structures and morphology of dinaphthothienothiophene (DNTT) thin films on highly oriented pyrolytic graphite, due to the incorporation of a polar chlorogallium phthalocyanine (ClGaPc) molecular layer at the interface, substitution of DNTT with alkyl side-chain-incorporated S-shaped DNTT (S-DNTT-C10), and thermal annealing, were investigated using photoelectron spectroscopic techniques to check the possibility of proper energy level alignment at the metal–organic interface, which is one of the key challenges to improve the charge transport in organic semiconductor-based devices. A significant modulation in the vacuum level (VL) and a small downward shift in the highest occupied molecular orbital (HOMO) level with an intermediate charge injection level (CIL) are evident in the DNTT thin film due to the incorporation of the ClGaPc layer at the interface. This is a clear signature of the molecular dipole layer (of well-ordered Cl-up orientated ClGaPc molecules)-induced realignment of the molecular energy levels of the DNTT thin films. On the other hand, a noticeable downward shift in the VL, a signature of an improvement in the bulk coverage, is evident in the S-DNTT-C10 film, which can be attributed to the presence of aliphatic hydrocarbons in the alkyl side-chain incorporated molecule. Furthermore, a double-peak-like HOMO level is evident in the S-DNTT-C10 film, which can be attributed to the two distinct orientations/arrangements of the molecules, one at the interface and other in the remaining part of the film. The formation of an intermediate CIL, through incorporation of a molecular dipole layer at the interface, is helpful to overcome the large hole injection barrier, while the enhancement of molecular coverage at the metal–organic interface and thereafter, through molecular engineering, is useful to increase the hole injection area, both of which are of immense importance in improving the device performances.



## 1. INTRODUCTION

Semiconductor-based devices have played a major part in the development of mankind. Silicon, germanium, and other conventional semiconductors have brought the world to our fingertips through revolution in modern technology. Further efforts are still on to improve and miniaturize modern devices based on such conventional semiconductors. At the same time, unconventional organic semiconductors are also becoming quite important due to their unique capabilities to form large-scale and flexible devices through easy processing. Extensive research is going on with these materials<sup>1–9</sup> in the form of organic thin-film transistors,<sup>10–13</sup> organic photovoltaics,<sup>14,15</sup> and organic light-emitting diodes<sup>16</sup> for their potential applications in electronic and optoelectronic industries as well as in medical devices.<sup>17</sup> Although these materials are very promising for future electronic and optoelectronic devices, there are some issues with these kinds of materials like low charge carrier mobility, poor environmental stability, and so on. Recently, some materials have been developed, which show

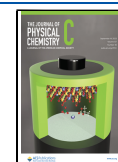
impressive charge carrier mobility and very good air and thermal stability. Dinaphtho[2,3-*b*:2',3'-*f*]thieno[3,2-*b*]thiophene (DNTT) and its derivatives are some of them.<sup>13,17–19</sup>

DNTT is a highly  $\pi$ -extended semiconducting molecule, consisting of six fused aromatic rings (two fused thiophene rings at the center and two fused benzene rings at both ends as shown in Figure 1),<sup>20,21</sup> having high ionization potential (IP  $\approx$  5.44 eV),<sup>18</sup> which makes it environmentally more stable than other similar class of molecules like pentacene (IP  $\approx$  4.85 eV),<sup>22</sup> and thus a subject of intense research. The interfacial molecular structure of DNTT and its evolution on noble

Received: June 19, 2023

Revised: July 27, 2023

Published: August 31, 2023



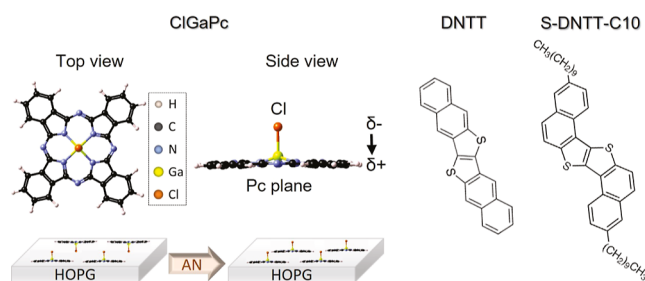


**Figure 1.** Molecular structure of ClGaPc, DNNT, and S-DNNT-C10 molecules. ClGaPc is a polar molecule and its dipole direction depends on its adsorption geometry on the substrate surface.

metallic surfaces were conscientiously studied, which revealed the surface texture-dependent molecular orientation.<sup>23</sup> The effect of gate-dielectric surface roughness on the charge transport property of DNNT layer was recently studied, which revealed roughness-dependent localized trap states.<sup>24</sup> A strong intermolecular interaction was also found to be present in this molecule on a Au surface, which has a clear impact on its molecular energy levels and charge transport-related parameters.<sup>25,26</sup>

The energy level alignment (ELA) at the metal–organic interface is a very important factor to improve the performance of an organic semiconductor-based device.<sup>27</sup> It is known that the energy level realignment is possible through various molecular energy level engineering techniques.<sup>28</sup> Incorporation of a molecular layer between a metal and an organic semiconducting layer is one such interesting tool to engineer the energy levels at the metal–semiconductor interface.<sup>29,30</sup> An interfacial molecular layer of polar molecule is of particular interest as it can form a net dipole moment through organization of the molecules in a particular orientation. The molecular dipole layer was found to form on the metal surface through controlled deposition and thermal annealing of the polar molecules, such as chlorogallium phthalocyanine (ClGaPc).<sup>31,32</sup> The resultant dipole direction of such a layer was, however, found to depend on the adsorption geometry of the molecules on that specific metal surface (as shown schematically in Figure 1).<sup>31,32</sup> Incorporation of such a molecular dipole layer, which can tune and/or align the molecular energy levels at the metal–DNNT interface, has not been studied so far. The coverage of the organic semiconductors, apart from the ELA, at the metal–organic interface, also plays an important role in improving the performance of the organic semiconductor-based device. Engineering of the semiconducting molecule itself can be an efficient way toward the betterment of the coverage and other structural parameters. Recently developed DNNT derivatives, namely, S-DNNT-C10,<sup>19</sup> with slightly modified DNNT structure and having alkyl side-chains on both sides of the main S-DNNT molecule (as shown schematically in Figure 1) can provide such opportunities, which needs to be looked into.

In this report, the evolution of electronic structures and morphology of DNNT thin films on highly oriented pyrolytic graphite (HOPG), due to the incorporation of a ClGaPc molecular layer at the interface, substitution of DNNT with S-DNNT-C10, and thermal annealing, were investigated using X-ray and ultraviolet photoelectron spectroscopic (XPS and UPS) techniques.<sup>33</sup> Indeed a realignment of the molecular energy levels, in general and a modulation in the vacuum level (VL), a downward shifted highest occupied molecular orbital

(HOMO) level, and an intermediate charge injection level (CIL) for overcoming large hole injection barrier ( $\phi_{\text{Br}}$ ), in particular, are evident in the DNNT/HOPG system due to the incorporation of the ClGaPc molecular layer. However, no appreciable chemical interaction is found at the interface. This is a clear signature of the molecular dipole layer (formed by ClGaPc molecules)-induced realignment of the molecular energy levels of DNNT thin films. On the other hand, a noticeable downward shift in the VL and a double-peak-like HOMO level are evident in the S-DNNT-C10 film. First one is a clear signature of aliphatic hydrocarbon (arising from alkyl side-chains of S-DNNT-C10 molecule) induced enhancement of wetting of the film, while the second one is related to the two different arrangements of the molecules: one at the interface and other in the remaining part of the film. The possible implications of such interesting changes in the energy levels and coverage of the DNNT thin films, due to the incorporation of a molecular dipole layer and/or due to the molecular engineering, on the DNNT-based electronic devices have been discussed.

## 2. EXPERIMENTAL DETAILS

The electronic structures of the DNNT molecular thin films were characterized using in situ XPS and UPS techniques in an ultra-high vacuum (UHV) chamber (Omicron Nanotechnology, of base pressure  $\sim 1.5 \times 10^{-9}$  mbar).<sup>26,32</sup> The UHV system was equipped with an EA125 hemispherical energy analyzer along with a UV and an X-ray light source for performing photoelectron spectroscopic experiments. A He gas discharge lamp (He I of energy 21.2 eV) was used as the UV light source for UPS measurements (corresponding energy resolution was  $< 0.1$  eV). A sample bias voltage of amount  $-6$  V was used to determine the higher binding energy cutoff (HBEC) during the UPS experiment. XPS experiments have been performed using a monochromatic X-ray source (Al  $K\alpha$  of photon energy 1486.6 eV) and the corresponding spectrometer resolution was  $\sim 0.8$  eV. All the data were collected keeping the samples at room temperature. The take-off angle of the photoelectrons was set at  $90^\circ$  for higher photoelectron yield.

HOPG was chosen as the substrate due to its non-reactive nature. Prior to the insertion of the HOPG substrate into the UHV chamber, its top layer was peeled off for getting a fresh and clean HOPG surface. Organic molecular thin films were grown in a high-vacuum deposition chamber (of base pressure  $\sim 1.0 \times 10^{-8}$  mbar), attached to the UHV characterization chamber, for controlled thin-film deposition, using the thermal evaporation technique. Highly pure ClGaPc (purity  $\approx 97\%$  from Sigma-Aldrich), DNNT (purity  $\approx 99\%$  from Sigma-Aldrich), and S-DNNT-C10 (purity  $> 99.5\%$  from TCI Chemicals) were purchased and used as it was. Thin films of ClGaPc, DNNT, and S-DNNT-C10 were deposited on the substrate by the thermal evaporation technique from quartz crucible-equipped Knudsen effusion cells. The substrate was kept at room temperature all the time during deposition. The deposition rate was kept at  $\sim 1 \text{ \AA min}^{-1}$  which was monitored by a quartz crystal microbalance. For the preparation of the DNNT/ClGaPc/HOPG system, a thin layer of ClGaPc (of nominal thickness  $\approx 3 \text{ \AA}$ ) was first deposited on HOPG and then annealed at  $150^\circ \text{C}$  for 4 h to get an ordered molecular dipole layer.<sup>32</sup> Subsequently, the DNNT layers of different cumulative nominal thickness ( $D_{\text{CN}} = 3, 6, 9, 16, \text{ and } 32 \text{ \AA}$ ) were deposited on it in steps and annealed at  $100^\circ \text{C}$  for 1 h

after each step of deposition. For the preparation of the S-DNTT-C10/HOPG system, S-DNTT-C10 layers of  $D_{\text{CN}} = 3, 6, 15, 30,$  and  $60 \text{ \AA}$  were deposited on HOPG in steps and annealed at  $110 \text{ }^\circ\text{C}$  for 1 h after each step of deposition. The deposited thin films of different thicknesses, before (AG\*) and after annealing (AN), were then characterized by XPS and UPS. C 1s core level of HOPG (of binding energy  $284.4 \text{ eV}$ ) was used as a reference level to calibrate the XPS spectra of the films.<sup>26,32</sup> The PeakFit, CasaXPS, and OriginPro software were used for analyzing the spectroscopic data. The well-known Shirley method was used for the XPS background subtraction, whereas the Gaussian–Lorentzian sum function was used to fit all the XPS core-level spectra.

### 3. RESULTS AND DISCUSSION

**3.1. UPS Study of DNTT/HOPG System.** The electronic structure of the DNTT/HOPG system was reported before,<sup>26</sup> which is discussed here briefly in order to understand the effect of the molecular dipole layer incorporation or molecular engineering on that system. No noticeable change in the HBEC or the VL is observed in the UPS spectra at the HBEC region of the DNTT/HOPG system with the increase in film thickness and with thermal annealing (as shown in Figure S1 of the Supporting Information). The lack of change of VL in the DNTT/HOPG system is due to the non-interacting nature of the interface.<sup>29,34</sup> This actually reflects the non-active nature of the HOPG surface and eliminates the possibility of formation of any interfacial dipole.<sup>26,32</sup> Such non-active nature of the HOPG surface toward organic molecules actually reduces the unintentional interaction at the interface, which is useful to study the molecular dipole-induced effect and thus makes it a perfect choice as a substrate.

On the other hand, the HOMO region of the UPS spectra (as shown in Figure S2 of the Supporting Information) shows a peak at around  $1.5 \text{ eV}$  in the  $3 \text{ \AA}$  thick film, which shifts slightly toward the higher binding energy side with the increase of the film thickness and also with thermal annealing. An appreciable increase in the peak intensity, especially for the  $3 \text{ \AA}$  thick film, was found due to the thermal annealing. It seems that in the as-grown films the interfacial coverage was small and the molecular ordering was less, while after thermal annealing the interfacial coverage increases and the ordering of the molecules improves to make the HOMO peak intense and sharp. Atomic force microscopy (AFM) images or topography of the DNTT film on HOPG, as reported before, however, suggests that the coverage of the DNTT molecular layer is very low and it gets even lower with thermal annealing.<sup>26</sup> These complementary results essentially suggest that the DNTT molecules adsorbed on the HOPG substrate in flat-lying orientation to form an interfacial layer and then form small dewetted domains of bulk crystalline structure due to the interfacial stress arising from the miss-match in the molecular orientation between the interfacial layer and the bulk crystalline domain layer. With thermal annealing, though the coverage of the interfacial layer increases but the coverage of the crystalline domains above it decreases.<sup>26</sup> This kind of molecular orientation was also observed in pentacene molecular thin films on the HOPG surface.<sup>29,35</sup> The  $\phi_{\text{bh}}$  in the  $3 \text{ \AA}$  DNTT/HOPG film was found around  $1.3 \text{ eV}$  and no significant change was observed due to the increase in the film thickness and also after thermal annealing. The threshold ionization potential ( $\text{IP}_{\text{th}}$ ) was observed at around  $5.8 \text{ eV}$  although the bulk IP of DNTT on Au surface was reported at

around  $5.44 \text{ eV}$ .<sup>18</sup> The higher  $\text{IP}_{\text{th}}$  of the DNTT/HOPG film can be attributed to the different molecular organization at the interface compared to the rest of the film.<sup>26</sup>

**3.2. UPS Study of the S-DNTT-C10/HOPG System.** The UPS spectra of the as-grown S-DNTT-C10 thin films of different thicknesses on the HOPG substrate are shown in Figure 2. No noticeable change in the HBEC or the VL was

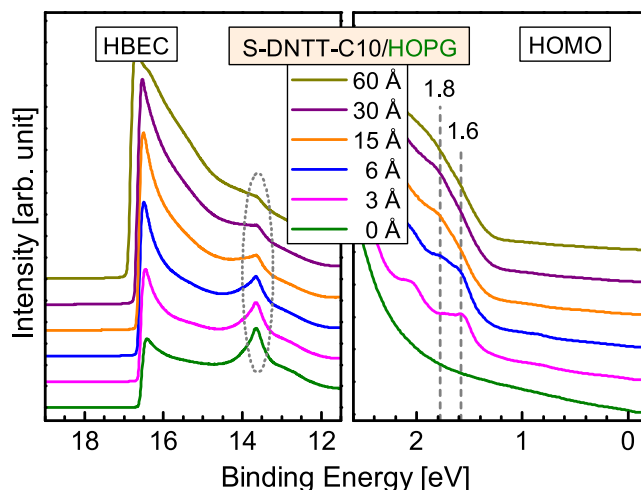


**Figure 2.** Evolution of the HBEC and HOMO regions of the UPS spectra of the as-grown (AG) S-DNTT-C10/HOPG system with S-DNTT-C10 layer thickness ( $D_{\text{CN}}$ ).  $\sigma^*$  band peak in the HBEC region and two peak-like feature in the HOMO region are indicated.

found in the S-DNTT-C10 films for thickness upto  $30 \text{ \AA}$ , which is due to the non-interacting nature of the S-DNTT-C10/HOPG interface, similar to that of the DNTT/HOPG interface. However, a finite change in the HBEC was evident in the  $60 \text{ \AA}$  thick film. Another noticeable change in the HBEC region of the S-DNTT-C10/HOPG is the peak intensity associated with the  $\sigma^*$  conduction band of the HOPG.<sup>29</sup> It was found that the intensity of this peak decreases significantly with the increase of film thickness and almost dies out for the  $60 \text{ \AA}$  thick film. This is a clear signature of the increase in the coverage of the film. That means the S-DNTT-C10 molecules, unlike the DNTT molecules, cover the HOPG surface very well. The hydrophobic alkyl side-chains of the S-DNTT-C10 molecule prefer and wet the HOPG surface (which is generally hydrophobic in nature), resulting in a film with better coverage. S-DNTT-C10 molecules were also found to wet the  $\text{SiO}_2/\text{Si}$  surface better than DNTT.<sup>19</sup> So, the molecules with alkyl side-chains show better wettability than the molecules without a side-chain. A finite negative VL shift (of  $\sim 0.3 \text{ eV}$ ), as observed in the film with higher thickness, is presumably due to its high coverage.

The UPS spectra in the HBEC region of the S-DNTT-C10 thin films of different thickness on HOPG substrate, before and after annealing, are shown in Figure 3. The evolution of the HBEC or the VL shift with thickness and thermal annealing (as shown in Figures S3 and S4 of the Supporting Information) suggests that the change is only prominent for the  $60 \text{ \AA}$  thick film. A maximum negative VL shift (of  $\sim 0.4 \text{ eV}$ ) is observed for the thick film after thermal annealing, suggesting the maximum coverage of the film. The UPS spectra in the HOMO region of the S-DNTT-C10 thin films of different thickness on the HOPG substrate, before and after annealing, are shown in Figure 4. A double peak-like feature of

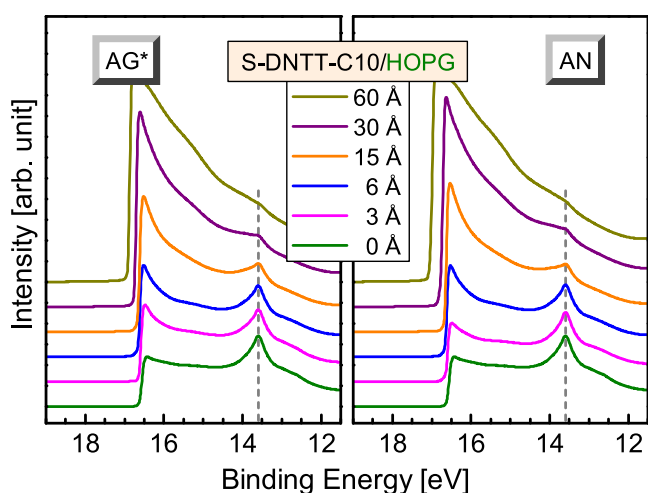


**Figure 3.** Evolution of the HBEC region of the UPS spectra of the S-DNTT-C10/HOPG system with S-DNTT-C10 layer thickness ( $D_{CN}$ ), before (AG\*) and after (AN) thermal annealing, after each step of deposition.  $\sigma^*$  band peak position is indicated by a dashed line.

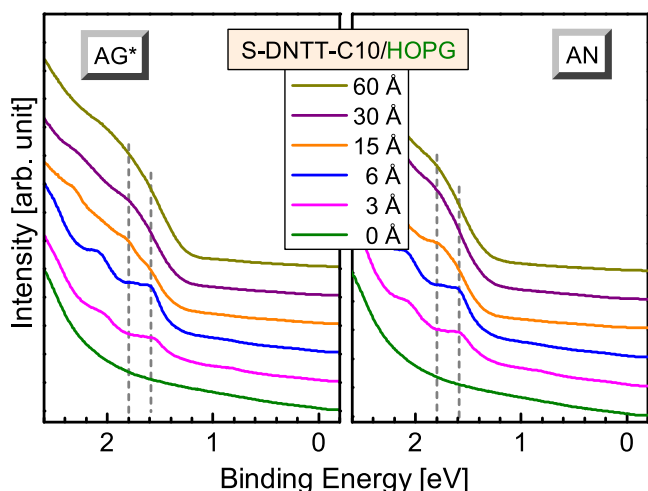


**Figure 4.** Evolution of the HOMO region of the UPS spectra of the S-DNTT-C10/HOPG system with S-DNTT-C10 layer thickness ( $D_{CN}$ ), before (AG\*) and after (AN) thermal annealing, after each step of deposition. HOMO band peak positions are indicated by dashed lines.

the HOMO level is observed here, though the addition of any insulating alkyl side-chains to an organic semiconducting molecule or a small change in the shape of the molecule is not expected to change its electronic structure a lot.<sup>36,37</sup> For the 3 Å thick film, the primary peak is observed at  $\sim 1.6$  eV and a faint secondary peak at  $\sim 1.8$  eV. No major effect of thermal annealing was observed in this case unlike the DNTT molecule. With the increase of film thickness, the intensity of the higher binding energy (secondary) peak increases compared to the lower binding energy (primary) peak. This result suggests that the molecular orientation in the top layer is different compared to that in the bottom interfacial layer. In the 3 Å thick film, most of the molecules adsorb on the HOPG surface with a distinct molecular orientation, possibly in flat-lying, similar to that observed for DNTT and pentacene molecules,<sup>26</sup> resulting in an intense lower binding energy peak in the HOMO level. A few molecules on top of it, with a very

different molecular orientation compared to that of the flat-lying molecules, probably form a bulk crystalline structure, to contribute in the faint higher binding energy peak. The bilayer separation along out-of-plane direction ( $d = 32$  Å) for the thick film of  $D_{CN} = 60$  Å, obtained from the X-ray diffraction (XRD) data (shown in Figure S5 of the Supporting Information), indicates the formation of bulk crystalline structure. With the increase of film thickness, most of the molecules adsorbed on top of the interfacial layer resulting in a gradual increase in the intensity of the higher binding energy HOMO peak compared to the lower binding energy one. The increasing randomness in the molecular orientation with the increase in film thickness causes a broadening of the HOMO peaks resulting in a broad unresolved double peak feature of the HOMO level. No significant change of the  $\phi_{Bh}$  was observed in these films compared to the DNTT films, which is well expected as no major change in the electronic structure takes place due to the addition of this alkyl side-chain, apart from a small change in its molecular conformation.

**3.3. UPS Study of DNTT/ClGaPc/HOPG System.** The UPS spectra, in the HBEC and the HOMO regions, of the 3 Å thick ClGaPc film on HOPG substrate, before and after thermal annealing (as shown in Figure S6 in the Supporting Information) give an idea about the formation of the molecular dipole layer.<sup>32</sup> As-grown 3 Å thick ClGaPc layer shows a two-peak convoluted HOMO level, one at 1.2 eV (corresponding to the Cl-up oriented molecules) and the other at 1.4 eV (corresponding to the bilayer stack of Cl-up and down oriented molecules). After thermal annealing, the higher binding energy peak got suppressed and the lower binding energy peak became more intense. This result suggests that initially ClGaPc molecules adsorbed in mixed (Cl-up and Cl-down) orientations but after annealing, most of them aligned themselves in Cl-up orientation to give rise to the corresponding HOMO peak only. A change in the HBEC that corresponds to the VL of an amount of around 0.2 eV was also observed after annealing the film. Such a transition in the molecular orientation, from mixed orientation to Cl-up orientation, gives rise to a net molecular dipole moment, which is evident from the shift in the VL (of  $\sim 0.2$  eV) due to thermal annealing, and confirms the formation of a molecular dipole layer of Cl-up oriented ClGaPc molecules on the HOPG surface. The formation of large islands of ClGaPc on HOPG, with a preferential alignment of Cl pointing upward, was also deduced before considering XPS and UPS data, large scale AFM images, and following the analogy found in the literature for ClGaPc and similar molecules.<sup>31,32,38</sup>

The HBEC region of the UPS spectra of the DNTT thin films of different thicknesses on the molecular dipole layer containing ClGaPc/HOPG substrate, before and after thermal annealing, are shown in Figure 5. An appreciable effect of the molecular dipole layer on the HBEC of the DNTT thin film was observed (also clearly evident from Figure S7 in the Supporting Information). A gradual negative VL shift of DNTT layer with deposition amount or thickness is evident (from Figure S8 in the Supporting Information). However, no noticeable change is observed after thermal annealing. Maximum VL shift ( $\sim 0.2$  eV) toward downward direction is observed for the 32 Å thick film. This kind of downward shift of the VL was not observed for the DNTT thin films on the HOPG surface. So, the downward shift of the VL in this case suggests some kind of charge reorganization at the DNTT/

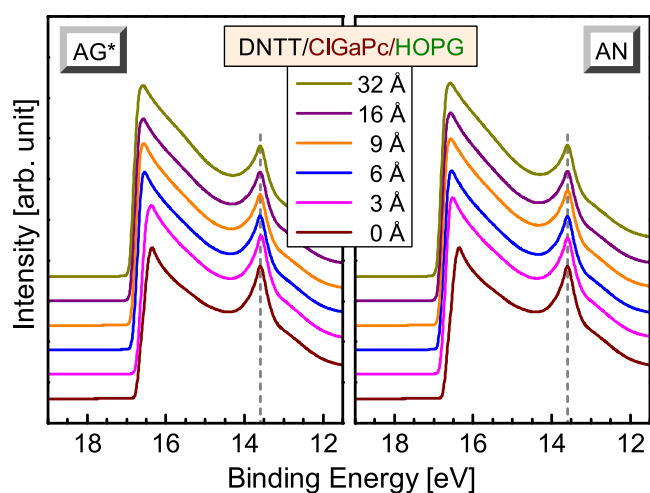


**Figure 5.** Evolution of the HBEC region of the UPS spectra of the DNTT/CiGaPc/HOPG system with DNTT layer thickness ( $D_{CN}$ ), before (AG\*) and after (AN) thermal annealing, after each step of deposition.  $\sigma^*$  band peak position is indicated by a dashed line.

CiGaPc interface, probably to compensate the effect caused by the molecular dipoles.

The HOMO regions of the DNTT/CiGaPc/HOPG thin films, before and after thermal annealing, are shown in Figure 6. A finite shift in the DNTT-related HOMO peak is observed

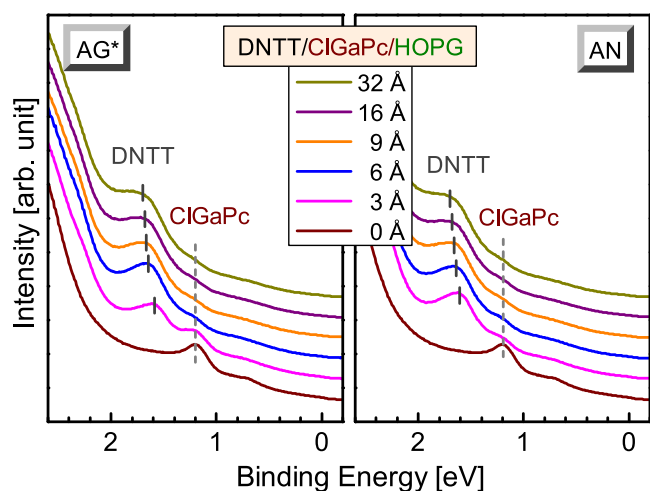


**Figure 6.** Evolution of the HOMO region of the UPS spectra of the DNTT/CiGaPc/HOPG system with DNTT layer thickness ( $D_{CN}$ ), before (AG\*) and after (AN) thermal annealing, after each step of deposition. HOMO bands corresponding to the DNTT and CiGaPc are indicated by dashed lines.

in the DNTT/CiGaPc/HOPG system compared to the DNTT/HOPG system, which went up to  $\sim 0.2$  eV for the thicker films. So, the molecular dipole layer is affecting the DNTT-related HOMO level apart from its VL, as mentioned before. Furthermore, an increment in the DNTT-related HOMO peak intensity is observed in the AG 3 Å thick film of DNTT on CiGaPc/HOPG compared to that on HOPG. This result suggests that the molecular dipole layer incorporated substrate not only tunes the molecular energy levels but also improves the wettability and/or the molecular ordering of the DNTT film at the interface. After annealing, the DNTT-related HOMO peak became more intense and the

CiGaPc-related HOMO peak got further suppressed. It is clear that the annealing improves the wettability and hence the coverage of the DNTT molecules, which makes the CiGaPc layer less visible by the photoelectrons, causing a very less intense CiGaPc-related HOMO peak. This phenomenon is also observed in the films with higher thickness. In the case of DNTT/HOPG films, the thermal annealing improves the coverage of the interfacial layer but not the remaining top part.<sup>26</sup> On the other hand, the molecular dipole layer itself improves the coverage of the DNTT layer, which got stimulated further by the thermal annealing. At the same time, it increases the  $\phi_{Bh}$  by shifting the DNTT-related HOMO level away from the substrate Fermi level. However, the presence of CiGaPc related HOMO level, in between, is important, which can play the role of an intermediate CIL for overcoming large  $\phi_{Bh}$ .

**3.4. XPS Study of DNTT/HOPG System.** The interfacial interaction of the DNTT/HOPG system, which was reported before,<sup>26</sup> is discussed here briefly, to understand the effect of the molecular dipole layer incorporation or molecular engineering on to it. The S 2p<sub>3/2</sub> peak (as shown in Figure S9 of the Supporting Information) was found at around  $163.9 \pm 0.1$  eV, independent of the film thickness. A major increase in the peak intensity was observed in the 3 Å thick film after annealing at 100 °C. This result was inferred as an increment of the overall crystallinity of the film and improved coverage and molecular ordering at the interfacial layer due to thermal annealing. A similar improvement was also observed in the 6 Å thick film deposited at a stretch (not shown here) after thermal annealing. However, for the cumulatively deposited film, this phenomenon was not visible. This result indicates that the maximum interfacial coverage can be achieved by simply thermal annealing the 3 Å thick film. The coverage of the molecular domains above this interfacial layer, that was observed after subsequent cumulative deposition, however, reduces due to thermal annealing (as evident from the S 2p<sub>3/2</sub> peak intensity and AFM results<sup>26</sup>).

**3.5. XPS Study of S-DNTT-C10/HOPG System.** The S 2p core level spectra of the S-DNTT-C10/HOPG thin films are presented in Figure 7 to understand any possible change in

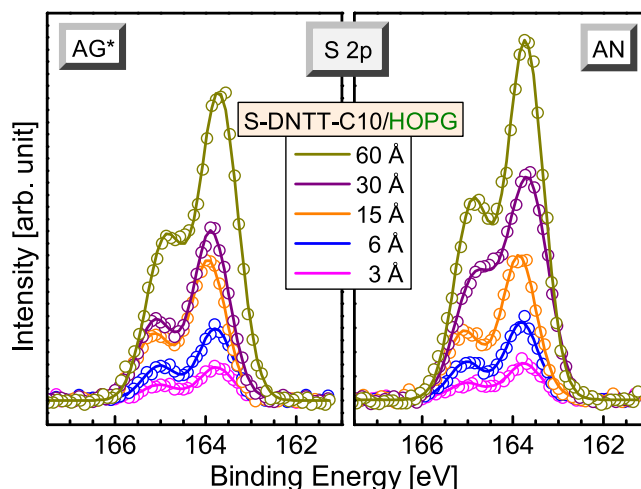


**Figure 7.** Evolution of the S 2p core level spectra of the S-DNTT-C10/HOPG system with S-DNTT-C10 layer thickness ( $D_{CN}$ ), before (AG\*) and after (AN) thermal annealing, after each step of deposition.

the interfacial interaction due to the introduction of the alkyl side-chain in the DNTT molecules. The S  $2p_{3/2}$  peak in the S-DNTT-C10/HOPG system was observed at around  $163.9 \pm 0.1$  eV similar to that in the DNTT/HOPG system, suggesting no appreciable change in the interfacial interaction even after incorporation of the alkyl side-chains, consistent with the inert nature of the HOPG surface. On the other hand, the evolution of the peak with thermal annealing for the S-DNTT-C10/HOPG system is found somehow different to that of the DNTT/HOPG system. Namely, a negligible increase of the peak intensity for the films with lower thickness, while a small increase for the films with higher thickness. The negligible increase indicates not much effect of annealing on the coverage of the interfacial molecular layer, which is well expected for the lower thickness films, where the interfacial coverage in the S-DNTT-C10/HOPG system, during deposition, is already high compared to that in the DNTT/HOPG system, as predicted from the UPS result. The small increase in the intensity with thermal annealing for the relatively thicker films suggests that though the annealing does not have enough effect on the molecules at the interfacial layer, it has an effect on the molecules above that layer to improve the coverage of the bulk crystalline-like domains in the S-DNTT-C10/HOPG system, unlike the DNTT/HOPG system. The better coverage of the S-DNTT-C10 layer compared to the DNTT layer on HOPG substrate is also evident from the better suppression of the C 1s peak (of the HOPG) for the thicker film of former molecules compared to the latter molecules (as shown in Figure S10 of the Supporting Information).

**3.6. XPS Study of DNTT/ClGaPc/HOPG System.** Atomic core level spectra of the DNTT thin films, of different cumulative nominal thickness, on ClGaPc/HOPG substrate before (AG\*) and after (AN) thermal annealing, are shown in Figure 8. S  $2p_{3/2}$  core level peak is found at  $163.9 \pm 0.1$  eV, without any noticeable change in its position with thickness, similar to the other two systems. The Ga 3s core level peak associated with the ClGaPc molecular layer is also observed in this region. The lack of change in that peak position (and also in the Ga  $2p_{3/2}$  core level spectra shown in Figure S11 of the Supporting Information) suggests the absence of any kind of

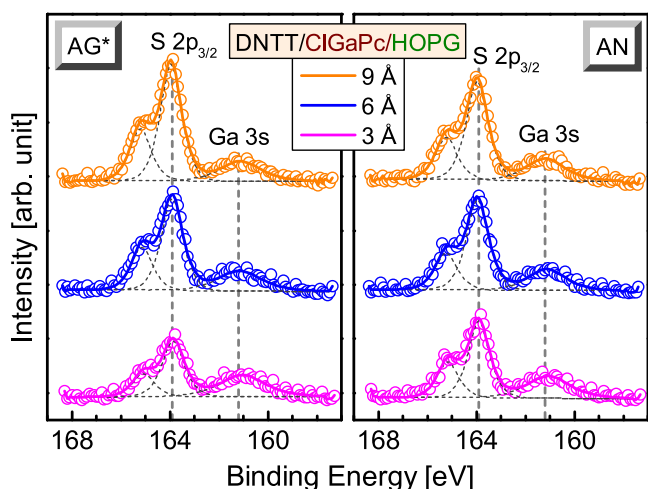


**Figure 8.** Evolution of the atomic core level spectra of the DNTT/ClGaPc/HOPG system with DNTT layer thickness ( $D_{CN}$ ), before (AG\*) and after (AN) thermal annealing, after each step of deposition.

chemical interaction at the DNTT/ClGaPc interface. A finite change in the intensity ratio of S 2p peak to Ga 3s peak, from  $\sim 2.3$  to  $\sim 3.2$ , is observed in the 3 Å thick film due to thermal annealing. However, the change is quite low compared to the DNTT film on HOPG. These results indicate that though there is an increase in the interfacial coverage of the DNTT molecule on ClGaPc/HOPG substrate after annealing, the increase is much less compared the DNTT molecule on the HOPG substrate, consistent with the UPS results. With the increase of film thickness, the intensity ratio increases suggesting an increase in the film coverage. However, lack of change in the intensity ratio for the thicker film after annealing indicates no further improvement in the coverage of the thicker film due to thermal annealing. Overall it suggests that the annealing has a finite effect on the DNTT/ClGaPc/HOPG system, which is less than that on the DNTT/HOPG system but greater than that on the S-DNTT-C10/HOPG system, validating the inference of the UPS results.

#### 4. OVERALL PICTURE AND SUMMARY

Let us now try to visualize the overall effect of the alkyl side-chain and the interfacial molecular dipole layer on the DNTT thin films. In order to do that, the evolution of the energy-level diagram and the corresponding molecular structure of the DNTT thin film on HOPG substrate due to the substitution of DNTT with S-DNTT-C10, incorporation of molecular dipole layer at the interface, and thermal annealing, as predicted from the complementary UPS and XPS techniques, are shown schematically in Figure 9.

**4.1. DNTT/HOPG System.** The lack of change in the VL due to the deposition of DNTT molecules on the HOPG surface indicates a non-interacting nature of the DNTT/HOPG interface and a very poor coverage of the bulk film. The HOMO level peak for the monolayer thick film is found at  $\sim 1.5$  eV, which moves slightly deeper for the multilayer thick films. The hole injection barrier for all the DNTT/HOPG films was found at  $\sim 1.3$  eV. A major increment in the HOMO level and S 2p core level peak intensities for the monolayer thick film after thermal annealing is related to the improvement in the coverage and/or ordering of the molecules at the interface, while relatively less increment for the multilayer thick films is related to the improvement in the ordering but not (rather decrement) in the coverage of the molecules in the rest of the films.

**4.2. S-DNTT-C10/HOPG System.** A two-peak-like HOMO level along with a small downward shift of the VL is evident in the S-DNTT-C10/HOPG system, especially for the multilayer thick film, though the hole injection barrier remains almost similar to that of the DNTT/HOPG system. The two-peak-like nature is the signature of two distinct molecular orientations of the molecules, one at the interfacial layer and other on top of it. The molecules at the interface seem to adsorb in a flat-lying orientation (to minimize the interfacial energy) to give rise the HOMO level closer to the Fermi level (prominent in the monolayer thick film) and the molecules on top of it are likely to be tilted significantly (as the flat-lying orientation is not preferred) to form a bulk crystalline phase (prominent in the multilayer thick film). The multilayer thick S-DNTT-C10 film shows a significant negative shift in the VL (of  $\sim 0.3$ – $0.4$  eV), unlike DNTT film, which is related to its higher coverage. This is also evident from the suppression of the  $\sigma^*$  conduction band peak (of the HOPG substrate) with film thickness. In the DNTT molecule, only aromatic

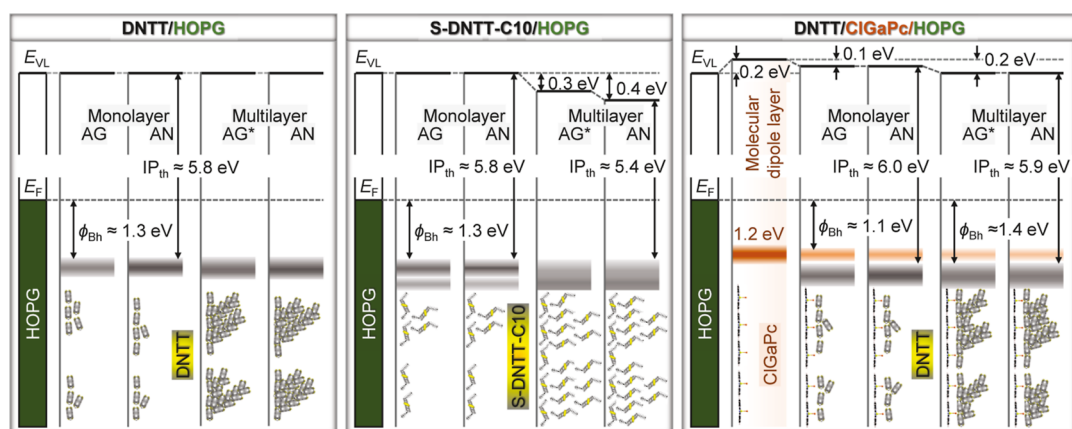


**Figure 9.** Evolution of energy-level diagram and possible orientation and/or organization of molecules at the DNTT/HOPG interface and thereafter, due to the incorporation of a molecular dipole layer of CiGaPc at the interface, substitution of DNTT with S-DNTT-C10, and thermal annealing, as predicted from complementary measurements.

hydrocarbons are present, while in the S-DNTT-C10 molecule, aliphatic hydrocarbons are also present. Such aliphatic hydrocarbons help in the wetting of the latter molecules. The absence of any chemical interaction at the interface is evident from the XPS results. The multilayer thick film also shows a further negative shift in the VL (and an increase in the S 2p peak intensity) with thermal annealing, which is related to the improvement in the bulk coverage of the film.

**4.3. DNTT/CiGaPc/HOPG System.** A CiGaPc molecular dipole layer shows a strong effect on the VL and also on the HOMO level of the DNTT molecular thin films. A modulation in the VL is due to the molecular dipole layer related positive shift (of  $\sim 0.2$  eV) and subsequent compensation related negative shift (of  $\sim 0.2$  eV). The interfacial molecular dipole layer shifts the DNTT related HOMO level further away from the Fermi level. This makes the  $\phi_{\text{Bh}}$  ( $\sim 1.4$  eV) in this system higher than the DNTT/HOPG system. However, the CiGaPc related HOMO level, is placed in between (Fermi level and DNTT HOMO level), which can act as an intermediate CIL to facilitate the charge transfer across the large hole injection barrier. The CiGaPc molecular dipole layer also increases the coverage of the interfacial DNTT layer that can be evident from the HOMO peak intensity of the monolayer thick film of DNTT on the CiGaPc/HOPG substrate compared to that on the HOPG substrate. After thermal annealing, the coverage of the interfacial DNTT layer on CiGaPc/HOPG improves a little bit, while that on HOPG improves appreciably as evident from the change in the intensity ratio of the HOMO peaks of DNTT and CiGaPc after thermal annealing and also from the XPS result. So, the molecular dipole layer shifts the whole energy level structure of DNTT further away from the Fermi level, and the thermal annealing has an intermediate effect on the DNTT/CiGaPc/HOPG system in the sense of improving the interfacial DNTT layer coverage.

In summary, the effects of alkyl side-chain and interfacial molecular dipole layer on the electronic structure of a model DNTT/HOPG system were obtained from the complementary UPS and XPS measurements. Such an electronic structure provides information not only on the energy levels and their alignments but also on the coverage and orientation/arrangement of the molecules in the film. A noticeable downward shift, observed in the VL of the S-DNTT-C10/HOPG system, indicates an improvement in the bulk coverage of the film, which is due to the presence of aliphatic

hydrocarbons in the alkyl side-chain incorporated molecule, while the double-peak-like HOMO level, observed in the same system, indicates two distinct orientations/arrangements of the molecules in the film; one at the interface (probably flat-lying) and the other in the remaining part (probably stand-up). A modulation in the VL and a small shift (away from the Fermi level) in the DNTT HOMO level, observed due to the incorporation of a molecular dipole layer at the DNTT/HOPG interface, indicate some kind of charge reorganization in the film to compensate the effect caused by the molecular dipole layer. This is a clear signature of a tunability of the DNTT-related HOMO level through the molecular dipole layer. However, in the present case, the effect is not positive in the sense it increases the hole injection barrier. This is related to the direction of the molecular dipole. By changing the direction of this molecular dipole (through changing the orientation of the CiGaPc molecules to Cl-down) and/or by selecting a proper combination of the molecular dipole layer (up- or down-dipole direction) and the organic semiconducting material (p- or n-type), it is possible to have a positive effect, which needs to be verified. In any way, the presence of a molecular dipole layer related HOMO level in the DNTT/CiGaPc/HOPG system is interesting as it can act as an intermediate CIL to overcome the large hole injection barrier, which will be useful to improve the charge transport properties of the DNTT-based devices.

## ■ ASSOCIATED CONTENT

### Supporting Information

The Supporting Information is available free of charge at <https://pubs.acs.org/doi/10.1021/acs.jpcc.3c04114>.

UPS and XPS spectra for the DNTT/HOPG system; UPS spectra of the CiGaPc thin layer on the HOPG substrate; estimated VL for the S-DNTT-C10/HOPG and DNTT/CiGaPc/HOPG systems; Ga 2p<sub>3/2</sub> core level spectra of the DNTT/CiGaPc/HOPG system; XPS survey spectra; and XRD pattern of a S-DNTT-C10 thin film on the HOPG substrate (PDF)

## ■ AUTHOR INFORMATION

### Corresponding Author

Satyajit Hazra – Saha Institute of Nuclear Physics, A CI of Homi Bhabha National Institute, Kolkata 700064, India;

orcid.org/0000-0001-5592-2078; Email: satyajit.hazra@saha.ac.in

## Authors

**Subhankar Mandal** – Saha Institute of Nuclear Physics, A CI of Homi Bhabha National Institute, Kolkata 700064, India;

orcid.org/0000-0001-8730-5920

**Souvik Jana** – Saha Institute of Nuclear Physics, A CI of Homi Bhabha National Institute, Kolkata 700064, India

**Saugata Roy** – Saha Institute of Nuclear Physics, A CI of Homi Bhabha National Institute, Kolkata 700064, India

**Md Saifuddin** – Saha Institute of Nuclear Physics, A CI of Homi Bhabha National Institute, Kolkata 700064, India;

orcid.org/0000-0003-1416-3081

Complete contact information is available at:

<https://pubs.acs.org/10.1021/acs.jpcc.3c04114>

## Notes

The authors declare no competing financial interest.

## ACKNOWLEDGMENTS

The authors thank Goutam Sarkar of SINP, Kolkata, India for his technical support. S.M. acknowledges the Council of Scientific & Industrial Research (CSIR), India and M.S. acknowledges the University Grant Commission (UGC), India, for providing research fellowships.

## REFERENCES

- (1) Wang, C.; Dong, H.; Hu, W.; Liu, Y.; Zhu, D. Semiconducting  $\pi$ -Conjugated Systems in Field-Effect Transistors: A Material Odyssey for Organic Electronics. *Chem. Rev.* **2012**, *112*, 2208–2267.
- (2) Kim, Y.-H.; Yoo, B.; Anthony, J. E.; Park, S. K. Controlled Deposition of a High-Performance Small-Molecule Organic Single-Crystal Transistor Array by Direct Ink-jet Printing. *Adv. Mater.* **2012**, *24*, 497–502.
- (3) Ostroverkhova, O. Organic Optoelectronic Materials: Mechanisms and Applications. *Chem. Rev.* **2016**, *116*, 13279–13412.
- (4) Saifuddin, M.; Mukhopadhyay, M.; Biswas, A.; Gigli, L.; Plaisier, J. R.; Hazra, S. Tuning the Edge-on Oriented Ordering of Solution-Aged Poly(3-hexylthiophene) Thin Films. *J. Mater. Chem. C* **2020**, *8*, 8804–8813.
- (5) McCuskey, S. R.; Chatsirisupachai, J.; Zeglio, E.; Parlak, O.; Panoy, P.; Herland, A.; Bazan, G. C.; Nguyen, T.-Q. Current Progress of Interfacing Organic Semiconducting Materials with Bacteria. *Chem. Rev.* **2021**, *122*, 4791–4825.
- (6) Roy, S.; Saifuddin, M.; Mandal, S.; Hazra, S. Stearic Acid Mediated Growth of Edge-on Oriented Bilayer Poly(3-hexylthiophene) Langmuir Films. *J. Colloid Interface Sci.* **2022**, *606*, 1153–1162.
- (7) Saifuddin, M.; Roy, S.; Mandal, S.; Hazra, S. Vibronic States and Edge-On Oriented  $\pi$ -Stacking in Poly(3-alkylthiophene) Thin Films. *ACS Appl. Polym. Mater.* **2022**, *4*, 1377–1386.
- (8) Zhang, Q.; Hu, W.; Sirringhaus, H.; Müllen, K. Recent Progress in Emerging Organic Semiconductors. *Adv. Mater.* **2022**, *34*, 2108701.
- (9) Saifuddin, M.; Biswas, A.; Roy, S.; Mandal, S.; Hazra, S. Nanoparticle Mediated Improved Crystallinity and Connectivity of Semiconducting Polymer Thin Films. *ACS Appl. Polym. Mater.* **2023**, *5*, 3359–3369.
- (10) Haas, S.; Takahashi, Y.; Takimiya, K.; Hasegawa, T. High-Performance Dinaphtho-Thieno-Thiophene Single Crystal Field-Effect Transistors. *Appl. Phys. Lett.* **2009**, *95*, 022111.
- (11) Zschieschang, U.; Ante, F.; Kälblein, D.; Yamamoto, T.; Takimiya, K.; Kuwabara, H.; Ikeda, M.; Sekitani, T.; Someya, T.; Nimoth, J. B.; et al. Dinaphtho[2,3-b:2',3'-f]thieno[3,2-b]-thiophene (DNNT) Thin-Film Transistors with Improved Performance and Stability. *Org. Electron.* **2011**, *12*, 1370–1375.
- (12) Melville, O. A.; Lessard, B. H.; Bender, T. P. Phthalocyanine-Based Organic Thin-Film Transistors: A Review of Recent Advances. *ACS Appl. Mater. Interfaces* **2015**, *7*, 13105–13118.
- (13) Huang, Y.; Gong, X.; Meng, Y.; Wang, Z.; Chen, X.; Li, J.; Ji, D.; Wei, Z.; Li, L.; Hu, W. Effectively Modulating Thermal Activated Charge Transport in Organic Semiconductors by Precise Potential Barrier Engineering. *Nat. Commun.* **2021**, *12*, 21.
- (14) Kim, D. Y.; So, F.; Gao, Y. Aluminum Phthalocyanine Chloride/C60 Organic Photovoltaic Cells with High Open-Circuit Voltages. *Sol. Energy Mater. Sol. Cells* **2009**, *93*, 1688–1691.
- (15) Mahato, S.; Puigdollers, J.; Voz, C.; Mukhopadhyay, M.; Mukherjee, M.; Hazra, S. Near 5% DMSO is the Best: A Structural Investigation of PEDOT:PSS Thin Films with Strong Emphasis on Surface and Interface for Hybrid Solar Cell. *Appl. Surf. Sci.* **2020**, *499*, 143967.
- (16) Cheng, C.-H.; Fan, Z.-Q.; Yu, S.-K.; Jiang, W.-H.; Wang, X.; Du, G.-T.; Chang, Y.-C.; Ma, C.-Y. 1.1  $\mu\text{m}$  Near-Infrared Electrophosphorescence from Organic Light-Emitting Diodes Based on Copper Phthalocyanine. *Appl. Phys. Lett.* **2006**, *88*, 213505.
- (17) Kuribara, K.; Wang, H.; Uchiyama, N.; Fukuda, K.; Yokota, T.; Zschieschang, U.; Jaye, C.; Fischer, D.; Klauk, H.; Yamamoto, T.; et al. Organic Transistors with High Thermal Stability for Medical Applications. *Nat. Commun.* **2012**, *3*, 723.
- (18) Yagi, H.; Miyazaki, T.; Tokumoto, Y.; Aoki, Y.; Zenki, M.; Zaima, T.; Okita, S.; Yamamoto, T.; Miyazaki, E.; Takimiya, K.; et al. Ultraviolet Photoelectron Spectra of 2,7-Diphenyl[1]benzothieno[3,2-b][1]benzothiophene and Dinaphtho[2,3-b:2',3'-f]thieno[3,2-b]-thiophene. *Chem. Phys. Lett.* **2013**, *563*, 55–57.
- (19) Yamaguchi, Y.; Kojiguchi, Y.; Kawata, S.; Mori, T.; Okamoto, K.; Tsutsui, M.; Koganezawa, T.; Katagiri, H.; Yasuda, T. Solution-Processable Organic Semiconductors Featuring S-Shaped Dinaphthothienothiophene (S-DNTT): Effects of Alkyl Chain Length on Self-Organization and Carrier Transport Properties. *Chem. Mater.* **2020**, *32*, 5350–5360.
- (20) Yamamoto, T.; Takimiya, K. Facile Synthesis of Highly  $\pi$ -Extended Heteroarenes, Dinaphtho[2,3-b:2',3'-f]chalcogenopheno[3,2-b]chalcogenophenes, and their Application to Field-Effect Transistors. *J. Am. Chem. Soc.* **2007**, *129*, 2224–2225.
- (21) Sánchez-Carrera, R. S.; Atahan, S.; Schrier, J.; Aspuru-Guzik, A. Theoretical Characterization of the Air-Stable, High-Mobility Dinaphtho[2,3-b:2'3'-f]thieno[3,2-b]-thiophene Organic Semiconductor. *J. Phys. Chem. C* **2010**, *114*, 2334–2340.
- (22) Sato, N.; Seki, K.; Inokuchi, H. Polarization Energies of Organic Solids Determined by Ultraviolet Photoelectron Spectroscopy. *J. Chem. Soc., Faraday Trans. 2* **1981**, *77*, 1621–1633.
- (23) Dreher, M.; Bischof, D.; Widdascheck, F.; Huttner, A.; Breuer, T.; Witte, G. Interface Structure and Evolution of Dinaphthothienothiophene (DNNT) Films on Noble Metal Substrates. *Adv. Mater. Interfaces* **2018**, *5*, 1800920.
- (24) Geiger, M.; Acharya, R.; Reutter, E.; Ferschke, T.; Zschieschang, U.; Weis, J.; Pflaum, J.; Klauk, H.; Weitz, R. T. Effect of the Degree of the Gate-Dielectric Surface Roughness on the Performance of Bottom-Gate Organic Thin-Film Transistors. *Adv. Mater. Interfaces* **2020**, *7*, 1902145.
- (25) Hasegawa, Y.; Yamada, Y.; Hosokai, T.; Koswattage, K. R.; Yano, M.; Wakayama, Y.; Sasaki, M. Overlapping of Frontier Orbitals in Well-Defined Dinaphtho[2,3-b:2',3'-f]thieno[3,2-b]-thiophene and Picene Monolayers. *J. Phys. Chem. C* **2016**, *120*, 21536–21542.
- (26) Mandal, S.; Roy, S.; Saifuddin, M.; Hazra, S. Hole-Injection Barrier Across the Intermolecular Interaction Mediated Interfacial DNNT Layer. *Appl. Surf. Sci.* **2022**, *597*, 153696.
- (27) Franco-Cañellas, A.; Duhm, S.; Gerlach, A.; Schreiber, F. Binding and Electronic Level Alignment of  $\pi$ -Conjugated Systems on Metals. *Rep. Prog. Phys.* **2020**, *83*, 066501.
- (28) Ishii, H.; Sugiyama, K.; Ito, E.; Seki, K. Energy Level Alignment and Interfacial Electronic Structures at Organic/Metal and Organic/Organic Interfaces. *Adv. Mater.* **1999**, *11*, 605–625.
- (29) Fukagawa, H.; Yamane, H.; Kataoka, T.; Kera, S.; Nakamura, M.; Kudo, K.; Ueno, N. Origin of the Highest Occupied Band

Position in Pentacene Films from Ultraviolet Photoelectron Spectroscopy: Hole Stabilization Versus Band Dispersion. *Phys. Rev. B: Condens. Matter Mater. Phys.* **2006**, *73*, 245310.

(30) Chen, H.; Zhang, W.; Li, M.; He, G.; Guo, X. Interface Engineering in Organic Field-Effect Transistors: Principles, Applications, and Perspectives. *Chem. Rev.* **2020**, *120*, 2879–2949.

(31) Gerlach, A.; Hosokai, T.; Duhm, S.; Kera, S.; Hofmann, O.; Zojer, E.; Zegenhagen, J.; Schreiber, F. Orientational Ordering of Nonplanar Phthalocyanines on Cu(111): Strength and Orientation of the Electric Dipole Moment. *Phys. Rev. Lett.* **2011**, *106*, 156102.

(32) Mandal, S.; Mukherjee, M.; Hazra, S. Evolution of Electronic Structures of Polar Phthalocyanine–Substrate Interfaces. *ACS Appl. Mater. Interfaces* **2020**, *12*, 45564–45573.

(33) Wang, Q.; Yang, J.; Gerlach, A.; Schreiber, F.; Duhm, S. Advanced Characterization of Organic–Metal and Organic–Organic Interfaces: From Photoelectron Spectroscopy Data to Energy-Level Diagrams. *J. Phys. Mater.* **2022**, *5*, 044010.

(34) Hill, I.; Rajagopal, A.; Kahn, A.; Hu, Y. Molecular Level Alignment at Organic Semiconductor–Metal Interfaces. *Appl. Phys. Lett.* **1998**, *73*, 662–664.

(35) Ozaki, H. Growth of Organic Ultrathin Films Studied by Penning Ionization Electron and Ultraviolet Photoelectron Spectroscopies: Pentacene. *J. Phys. Chem. C* **2000**, *113*, 6361–6375.

(36) Izawa, T.; Miyazaki, E.; Takimiya, K. Solution-Processible Organic Semiconductors Based on Selenophene-Containing Heteroarenes, 2,7-Dialkyl[1]benzoselenopheno[3,2-*b*] [1]-benzoselenophenes (C<sub>n</sub>-BSBSs): Syntheses, Properties, Molecular Arrangements, and Field-Effect Transistor Characteristics. *Chem. Mater.* **2009**, *21*, 903–912.

(37) Schott, S.; McNellis, E. R.; Nielsen, C. B.; Chen, H.-Y.; Watanabe, S.; Tanaka, H.; McCulloch, I.; Takimiya, K.; Sinova, J.; Sirringhaus, H. Tuning the Effective Spin-Orbit Coupling in Molecular Semiconductors. *Nat. Commun.* **2017**, *8*, 15200.

(38) Ueno, N.; Kera, S.; Sakamoto, K.; Okudaira, K. K. Energy band and Electron-Vibration Coupling in Organic Thin Films: Photoelectron Spectroscopy as a Powerful Tool for Studying the Charge Transport. *Appl. Phys. A* **2008**, *92*, 495–504.